JACS
JOURNAL OF THE AMERICAN CHEMICAL SOCIETY

Article

pubs.acs.org/JACS

Vibronic Dynamics of the Ultrafast all-*trans* to 13-*cis* Photoisomerization of Retinal in Channelrhodopsin-1

Christoph Schnedermann,[†,∥] Vera Muders,[‡,∥] David Ehrenberg,[§] Ramona Schlesinger,[‡] Philipp Kukura,[*,†] and Joachim Heberle[*,§]

[†]Physical and Theoretical Chemistry Laboratory, University of Oxford, South Parks Road, Oxford OX1 3QZ, United Kingdom
[‡]Genetic Biophysics, Department of Physics, and [§]Experimental Molecular Biophysics, Department of Physics, Freie Universität Berlin, Arnimallee 14, 14195 Berlin, Germany

Supporting Information

ABSTRACT: Channelrhodopsins are light-gated ion channels with extensive applications in optogenetics. Channelrhodopsin-1 from *Chlamydomonas augustae* (*Ca*ChR1) exhibits a red-shifted absorption spectrum as compared to Channelrhodopsin-2, which is highly beneficial for optogenetic application. The primary event in the photocycle of *Ca*ChR1 involves an isomerization of the protein-bound retinal chromophore. Here, we apply highly time-resolved vibronic spectroscopy to reveal the electronic and structural dynamics associated with the first step of the photocycle of *Ca*ChR1. We observe vibrationally coherent formation of the P_1 intermediate exhibiting a twisted 13-*cis* retinal with a 110 ± 7 fs time constant. Comparison with low-temperature resonance Raman spectroscopy of the corresponding trapped photoproduct demonstrates that this rapidly formed P_1 intermediate is stable for several hundreds of nanoseconds.

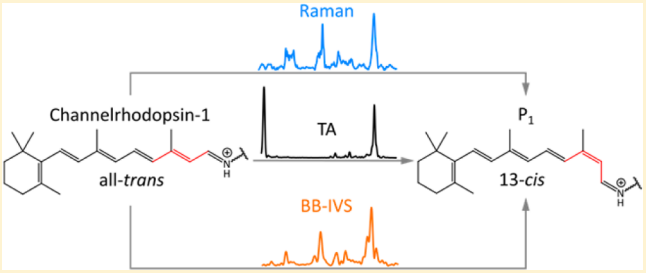

INTRODUCTION

Photoreceptors form an important class of membrane proteins with a wide range of functionalities such as visual signaling, proton pumping, and ion channeling.[1−3] Channelrhodopsins, which act as light-activated cation channels, have recently received great attention due to their enormous potential in optogenetics, an emerging field where photosensory proteins trigger a physiological response with light. Most prominently, channelrhodopsins are used in neuroscience to depolarize specific nerve cells upon light activation.[3,4] Originally, channelrhodopsins are located in the eyespot of green flagellate algae to mediate phototaxis[5] and can be divided into channelrhodopsin-1 (ChR1) and channelrhodopsin-2 (ChR2) on the basis of their structural and mechanistic differences.[6,7] Channelrhodopsin-2 from *Chlamydomonas reinhardtii* (*Cr*ChR2) is mostly used in optogenetics[8] and has been subject to a range of spectroscopic studies on the intermediates contributing to the photocycle.[7,9−12]

Much less is known about the dynamics of Channelrhodopsin-1 from *Chlamydomonas reinhardtii* (*Cr*ChR1), largely due to the difficulties associated with overexpression to obtain sufficient protein quantities for biophysical analysis. In contrast, channelrhodopsin-1 derived from *Chlamydomonas augustae* (*Ca*ChR1) can be heterologously expressed in large quantities in the yeast *Pichia pastoris*.[4,11] Moreover, *Ca*ChR1 has two desirable features for optogenetic application: (i) slower inactivation under continuous illumination and (ii) a red-shifted absorption maximum allowing for deeper penetration of the excitation light into biological tissue.[4]

*Ca*ChR1 exhibits a heterogeneous ground-state population of chromophore isomers comprised of 30% 13-*cis* to 70% all-*trans* retinal with a protonated Schiff base and an absorption maximum at 518 nm.[11] The photocycle of *Ca*ChR1 has been analyzed using time-resolved UV/vis, resonance Raman, and FT-IR spectroscopy.[11,13−15] Photoexcitation results in an early P_1 intermediate, which exhibits a red-shift in absorbance to 560 nm. This P_1 intermediate is followed by the long-lasting P_2 intermediate absorbing at 380 nm, whose rise time matches the millisecond lifetime of the passive cation current. Despite the fact that a red-shifted P_3 intermediate was detected in *Cr*ChR2, no such intermediate seems to be present in the photocycle of *Ca*ChR1.[15,16] Here, mainly the P_2 intermediate accumulates under continuous illumination at room temperature, facilitating the biophysical analysis of the conductive state in *Ca*ChR1.

Resonance Raman spectroscopy revealed that the P_2 intermediate consists of 13-*cis* retinal with a deprotonated Schiff base.[11] Additionally, large conformational as well as hydrogen-bonding changes of carboxylic groups, cysteine side chains, and of a dangling water molecule were detected between the closed and the open states of *Ca*ChR1 via FT-IR difference spectroscopy.[16] After channel closure, time-resolved IR spectroscopy revealed ongoing conformational changes in the P_4 intermediate.[16]

The key structural changes occurring directly after photoexcitation, however, are poorly understood as structural

Received: November 23, 2015
Published: March 21, 2016

DOI: 10.1021/jacs.5b12251
J. Am. Chem. Soc. 2016, 138, 4757−4762

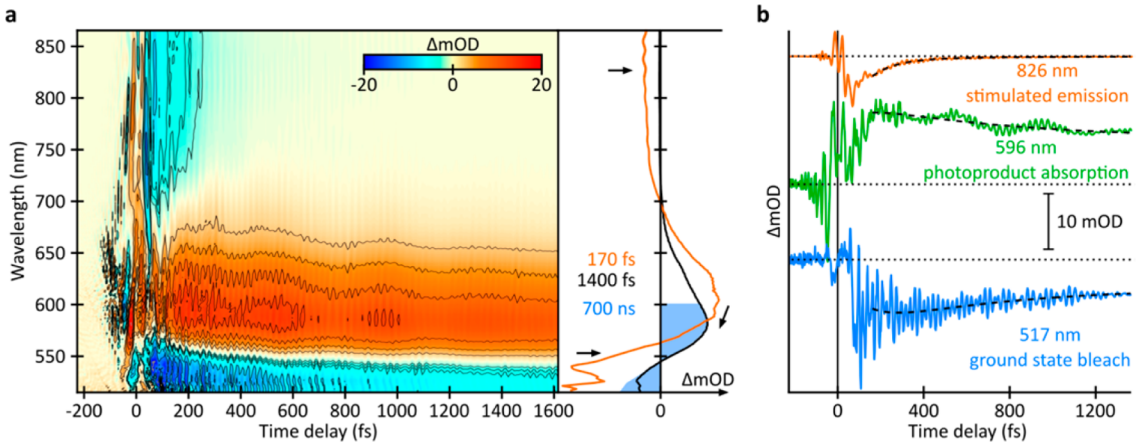

Figure 1. Ultrafast vibronic dynamics of *Ca*ChR1. (a) Transient absorption map of *Ca*ChR1 employing a visible 8 fs pump pulse centered at 560 nm and a chirped broadband whitelight continuum probe pulse (500−900 nm, 4.5 fs transform limit). Early coherent artifact contributions (−100 to 100 fs) have been subtracted for clarity. Selected transient absorption spectra at 170 fs (orange) and 1400 fs (black) illustrating the rapid initial dynamics are shown on the right with arrows indicating spectral changes with time. A flash photolysis spectrum obtained at 700 ns pump−probe delay (blue) suggests no significant spectral evolution over several hundreds of nanoseconds after the initial fast response is complete. (b) Selected transients demonstrating the dynamic characteristics of the vibronic transients with exponential fits (dashed black). Fitting was restricted to time delays >140 fs to avoid residual contributions from the coherent artifact.

information on the early photocycle of *Ca*ChR1 is restricted to photointermediates trapped under cryogenic conditions.[14] The typical isomerization times for photoexcited rhodopsins vary depending on the underlying change, the overall environment, and other factors.[17,18] The most commonly studied all-*trans* to 13-*cis* isomerization in bacteriorhodopsin occurs in ∼500 fs.[17,19,20] The same transformation in *Cr*ChR2 has been assigned to a lifetime of 600 fs,[9,21] while in the related *Anabaena* sensory rhodopsin (ASR) it proceeds with a time constant of ∼750 fs.[22,23] In contrast, the reverse isomerization in ASR is much faster with a time constant of 170 fs,[23] while the 11-*cis* to all-*trans* isomerization in visual rhodopsin reaches essentially ballistic dynamics with a completed isomerization within 200 fs.[24−26] Contrary to this trend, *Ca*ChR1 has been proposed to show a ∼100 fs time constant for an all-*trans* to 13-*cis* isomerization.[27]

Here, we combine high time-resolution transient absorption spectroscopy, time-domain broadband impulsive vibrational spectroscopy (BB-IVS),[19,26,28−30] and low-temperature resonance Raman spectroscopy to characterize the vibronic dynamics of the all-*trans* retinal chromophore in *Ca*ChR1 during the primary photoisomerization event. Although the kinetics of this process have been recently reported using ultrafast UV/vis spectroscopy, the structural dynamics remain uncharacterized.[27] We show that *Ca*ChR1 undergoes a rapid photoisomerization to the first stable P_1 intermediate with 13-*cis* retinal with an exponential time constant of 110 fs, which appears to persist for several hundreds of nanoseconds.

RESULTS AND DISCUSSION

Following photoexcitation of *Ca*ChR1 with an 8 fs pulse centered at 560 nm, we observe ground-state bleaching around 520 nm partially overlapped with a red-shifted photoinduced absorption band at 600 nm and a rapidly decaying stimulated emission band at 850 nm similar to the spectral dynamics reported for bacteriorhodopsin (Figure 1a).[19,20,31] The stimulated emission band has decayed completely 500 fs after photoexcitation, while the photoinduced absorption and ground-state bleach bands persist and decay on a slower time scale accompanied by a blue-shift and narrowing of the photoinduced absorption band. A global fitting routine employing an offset and two exponential functions is sufficient to describe the decay dynamics for time delays >140 fs, chosen to avoid contamination by coherent artifact contributions.[28] The first time constant (110 ± 7 fs) correlates with the rapid decay of the stimulated emission, while the second time constant (580 ± 40 fs) is predominantly related to the spectral blue-shift of the ground-state bleach and photoinduced absorption contributions as indicated in Figure 1a (orange and black transient spectra). The transient absorption spectrum at 1400 fs appears almost identical to a spectrum recorded at a time delay of 700 ns using flash photolysis, suggesting that the formation of the previously assigned intermediate, P_1,[27] completes on a subpicosecond time scale.

The measured photodynamics of *Ca*ChR1 are in excellent agreement with previously reported transient absorption measurements probed from 430 to 700 nm by Stensitzki et al.[27] In their work, the authors assign the ground-state absorption maxima of *Ca*ChR1 with all-*trans* and 13-*cis* chromophore to ∼540 and ∼480 nm, respectively. The observed transient dynamics in our experiment are hence dominated by photoexcited all-*trans* with only minor contribution from photoexcited 13-*cis* (Figure 1). To further verify this assignment, we repeated the experiment at different excitation wavelengths from 530 to 590 nm, which yielded no significant changes in the transient dynamics and spectra (Figure S1). In particular, the observed wavelength independence on the stimulate emission band at 850 nm strongly supports the notion that the main contributor to the transient dynamics is all-*trans*. Importantly, our ability to directly observe the stimulated emission decay at 850 nm enables us to assign the excited-state decay of all-*trans* to the shortest observed time constant of 110 fs, suggesting an ultrafast isomerization process, in contrast to recent reports on ChR2 attributing the shortest time constant to an excited-state reorganization.[9]

Closer examination of the individual transients (Figure 1b) reveals that the dynamics of the dominant transient absorption features are modulated by coherent oscillations, particularly pronounced in the photoinduced absorption and ground-state

DOI: 10.1021/jacs.5b12251
J. Am. Chem. Soc. 2016, 138, 4757−4762

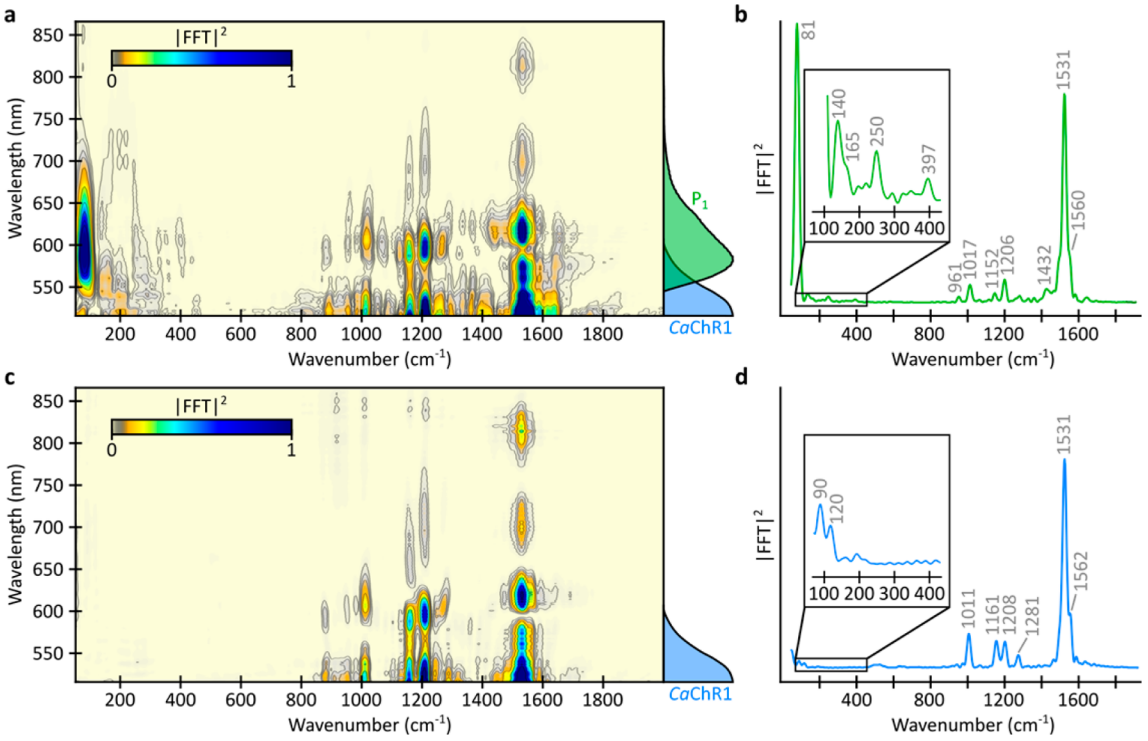

Figure 2. Time-domain impulsive vibrational Raman spectroscopy on *Ca*ChR1. (a) Wavelength-resolved Fourier-transform power map of *Ca*ChR1 obtained with a resonant 8 fs pump pulse centered at 560 nm. Representative absorption spectra of the photoproduct P_1 (green) and ground state (blue) are shown for comparison. (b) Spectral average over the low-energy side of P_1 (620−680 nm) showing strong activity in the low-frequency region <500 cm^{-1}. (c) Wavelength-resolved Fourier-transform power map of *Ca*ChR1 obtained with a 9 fs off-resonant pump pulse centered at 800 nm providing exclusively ground-state contributions. The ground-state absorption spectrum is shown for comparison. (d) Spectral average over the same probe region as in (a) lacking all major activity in the low-frequency region and at 961 cm^{-1}. We remark that the exact frequencies in the low-frequency region change depending on the Fourier transform parameters due to time-signal interference effects.

bleach band as previously reported for bacteriorhodopsin and visual rhodopsin.[19,24,26] The origin of the vibrational coherences is impulsive generation of nuclear wavepackets by the excitation pulse.[28,32−34] After subtraction of the slowly varying electronic dynamics, a Fourier transform of the residual coherent oscillations reveals the wavelength-dependent impulsive Raman spectra of the system (Figure 2a). The Fourier intensities decrease toward the near-IR with maxima close to the ground state and photoinduced absorption bands in line with previous reports.[26] We find strong contributions in the low-frequency region (<500 cm^{-1}) with dominant modes at 81 cm^{-1} and in the hydrogen wagging (~960 cm^{-1}), CH_3 rocking (~1010 cm^{-1}), C−C (~1200 cm^{-1}), and C═C (~1530 cm^{-1}) stretching regions (Figure 2b).[11]

A transient absorption experiment employing a short resonant pump pulse generates both ground- and excited-state vibrational coherences, leading to a superposition of spectral features. While a spectral nodal analysis[35,36] would be in general sufficient to assign the origin of the vibrational coherence, the broad spectral signatures in *Ca*ChR1 complicate the analysis for modes >500 cm^{-1}, which form the main focus of this work (see Figure S6 for a discussion on low-frequency modes). Instead, to identify vibrational coherences arising from photoexcited molecules, we repeated the experiment under identical conditions except for the use of an off-resonant pump pulse centered at 800 nm (9 fs) generating exclusively ground-state vibrational coherences, as described in detail previously.[30,37] The resulting impulsive Raman map reveals intense coherence activity in the hydrogen wagging, CH_3 rocking, and C−C and C═C stretching regions with an almost identical wavelength-dependence as under resonant conditions, while lacking all activity in the low-frequency region (Figure 2c). Closer inspection reveals that off-resonant excitation generates less coherence activity around the photoinduced absorption band at 600 nm, providing evidence for a vibrationally coherent formation of the P_1 intermediate as reported for visual rhodopsin.[38] This is further emphasized in a comparison of the spectral average at the low-energy side of the P_1 absorption spectrum from 620 to 680 nm. We find altered relative intensities of the fingerprint bands >800 cm^{-1} upon resonant excitation and an additional band at 961 cm^{-1}, which forms a sensitive marker band of a twisted retinal geometry (compare Figure 2d and b).[39,40] The observation of isomerized photoproduct vibrational coherences in combination with the apparent ultrafast decay dynamics of the stimulated emission band at 850 nm (Figure 1) supports the notion that the P_1 state with 13-*cis* retinal is indeed formed with a time constant of 110 fs, as previously assigned.[27] Solely on the basis of transient absorption spectra, such an assignment would be rather complicated due to the possibility of overlapping excited-state absorption features, often found in similar rhodopsins.[17,41]

To validate this assignment with structural sensitivity, we carried out room-temperature broadband impulsive vibrational spectroscopy (BB-IVS)[28] to determine the configuration of the molecular species formed by photoexcitation (Figure 3, orange spectrum). To this end, we photoexcited the system with an actinic pulse centered at 515 nm (200 fs) followed after 1 ps by an impulsive pulse centered at 800 nm (9 fs) to generate vibrational coherences directly in the photoproduct. Subtracting the vibrational coherences obtained in the presence and

DOI: 10.1021/jacs.5b12251
J. Am. Chem. Soc. 2016, 138, 4757−4762

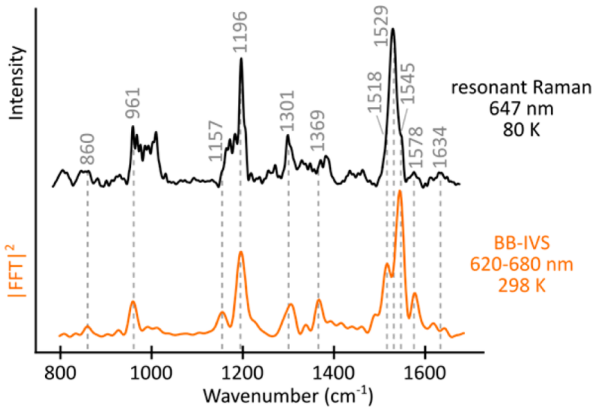

Figure 3. Resonance Raman spectra of the P_1 intermediate of *Ca*ChR1. Top: Low-temperature (80 K) resonance Raman spectrum of the primary photoproduct, P_1, obtained at 647 nm following photoexcitation at 514 nm. Bottom: Broadband impulsive vibrational (BB-IVS) spectrum of the P_1 intermediate recorded 1 ps after excitation at 515 nm (200 fs) using a 9 fs pump pulse centered at 800 nm. The BB-IVS spectral intensities are corrected for finite time resolution[17] and averaged over the low-energy side of the photoproduct absorption band (620−680 nm). Vertical dashed lines indicate matching frequencies and are labeled accordingly. In particular, the bands at 860, 961, 1196, and 1301 cm^{-1} are sensitive marker bands for the distorted 13-*cis* configuration of retinal in the photoproduct state.[39,40]

absence of the actinic pump pulse (Figure S2),[28] followed by Fourier transformation and spectral averaging from 620 to 680 nm, subsequently retrieves the photoproduct Fourier power spectrum 1 ps after photoexcitation (Figure 3, orange spectrum). The time delay was chosen to avoid generation of ground-state vibrational coherence by the impulsive pulse via the stimulated emission transition. We remark that at this time delay, the system is still cooling (Figure 1a). The BB-IVS spectrum will thus be composed of some vibrationally hot reactant and P_1 intermediate, which can lead to differences when compared to a pure P_1 Raman spectrum. A more detailed analysis is given in Figure S2.

In addition, we trapped the P_1 state at cryogenic temperatures (80 K) to perform resonance Raman spectroscopy with photoexcitation at 514 nm. Upon subtraction of the ground-state spectrum recorded in the absence of photoexcitation under otherwise identical conditions (Figure S3), we obtain the Raman spectrum of the P_1 state recorded under preresonant conditions (pRR) using continuous-wave excitation at 647 nm (Figure 3, black spectrum). Under these continuous excitation conditions, we cannot exclude minor contributions of a possible 13-*cis* photocycle product. The frequencies of the Raman bands are in close agreement with those observed by FT-IR difference spectroscopy[14] as deduced from the comparison of the latter with the difference Raman spectrum (Figure S4).

We find good agreement between the pRR and BB-IVS spectra supporting our earlier structural assignment of a 13-*cis* configuration for P_1. In particular, the hydrogen-wagging bands at 860 and 961 cm^{-1} are sensitive markers for a distorted retinal conformation. Furthermore, the bands in the C−C stretching region at 1157, 1196 cm^{-1} and in the CH_3 rocking region at 1301 cm^{-1} indicate that the retinal chromophore exhibits a 13-*cis* configuration.[39,40] The C═N−H stretching vibration of the retinal Schiff base is assigned to the band at 1634 cm^{-1} for the P_1 state at 80 K (compare to 1646 cm^{-1} for the initial ground state[11]). In conclusion, the occurrence of all of these marker bands provides solid evidence that the initial photoisomerization from all-*trans* to 13-*cis* retinal in *Ca*ChR1 occurs on a subpicosecond time scale.

Irrespective of the different spectral resolutions in the two experiments, we observe small frequency shifts between BB-IVS and pRR spectra (Figure 3), which may arise from different P_1 species measured at room and cryogenic temperatures. Such deviations are well-known for the various K states in the initial photoreaction of bacteriorhodopsin[42,43] and are related to differences in the conformation of the retinal chromophore and the structure of the surrounding binding pocket. In addition, BB-IVS and pRR spectra are expected to show further differences, particularly in regions where reactant and P_1 modes overlap strongly.[28,30] The reason is that the pRR spectrum reveals the true 13-*cis* Raman spectrum, while BB-IVS records the spectrum 1 ps after photoexcitation. This results in different subtraction performances in particular in congested frequency areas, like the C═C stretching region. However, despite all differences, both techniques have in common that the Raman activity in key marker modes increases upon photoexcitation, supporting an assignment to 13-*cis* retinal (Figures S2 and S3).

The structural assignment of the P_1 state allows us to explain the appearance of the direct excitation Fourier spectrum (Figure 2b). Low-frequency modes in *Ca*ChR1 are strongly enhanced upon photoexcitation. Such low-frequency modes can also be found in the closely related proteins bacteriorhodopsin and visual rhodopsin[17,19,44] as well as in the all-*trans* chromophore in solution.[45−47] It is the remarkably enhanced intensity observed for *Ca*ChR1, which indicates that the reaction must proceed extremely quickly along low-frequency coordinates, rendering *Ca*ChR1 striking similar to visual rhodopsin.[26,38]

Such behavior is characteristic for an isomerization coordinate comprising a number of low-frequency retinal backbone modes, which is crucial to obtain a controlled photoisomerization reaction capable of dissipating the excess photon energy rapidly. As a consequence, large low-frequency coherence activities arise, because low-frequency modes provide an internal energy sink for excess excitation energy for ultrafast processes on a subpicosecond time scale.[48,49] High-frequency modes (>800 cm^{-1}) are dominated by ground-state modes (Figure 2d, 1208, 1531 cm^{-1}), rendering it challenging to make a confident structural assignment. In contrast, BB-IVS (Figure 3, orange spectrum) significantly suppresses this background and confirms that the spectral differences are caused by the photoisomerization reaction forming a 13-*cis* intermediate with pronounced marker bands for a distorted 13-*cis* retinal such as the hydrogen wagging (860 and 961 cm^{-1}), the C−C stretching (1196 cm^{-1}), and the CH_3 rocking (1300 cm^{-1}) modes. In particular, the presence of the 961 cm^{-1} marker bands in the BB-IVS spectrum at 1 ps, the low-temperature pRR spectrum (Figure 3), and the direct excitation Fourier spectrum (Figure 2b) provides evidence for a P_1-like 13-*cis* retinal structure being generated with a time constant of 110 fs.

Combining these experimental results, we can assign the initial steps in the photocycle of *Ca*ChR1 (Figure 4). Photon absorption at 515−560 nm preferentially excites all-*trans* chromophores to the first excited electronic state[27] followed by rapid relaxation to an excited-state plateau characterized by a stimulated emission band at 850 nm, strikingly similar to the

DOI: 10.1021/jacs.5b12251
J. Am. Chem. Soc. 2016, 138, 4757−4762

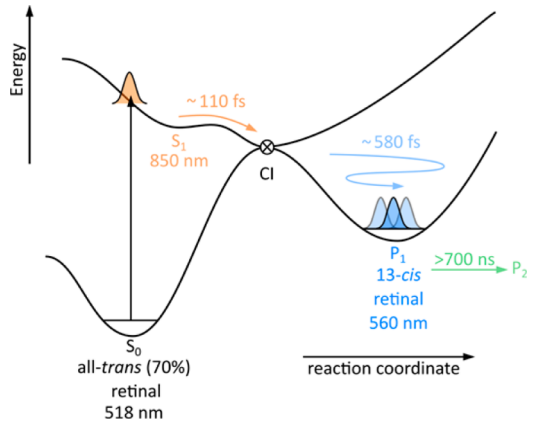

Figure 4. Potential energy diagram for the primary isomerization event in *Ca*ChR1. Photoexcitation at the absorption maximum (518 nm) promotes predominantly all-*trans* molecules to a short-lived (110 fs) excited state characterized by a stimulated emission band at 850 nm. After crossing back to the ground-state potential energy surface through a conical intersection (CI), back reversion to the reactant (not indicated) and photoproduct formation occurs. Subsequent cooling with a 580 fs time constant relaxes the molecules leading to the formation of a P_1 intermediate that is stable for several hundred nanoseconds.

observations made in bacteriorhodopsin.[19] On the basis of the similarity in photodynamics to bacteriorhodopsin, we propose a small excited-state barrier for *Ca*ChR1, most likely of dynamic origin leading to a flat excited-state plateau, as was recently proposed theoretically (Figure S5).[50,51] The structure associated with this plateau is most likely pretwisted along the 13-*trans* bond of retinal in analogy to bacteriorhodopsin, but due to the extremely short lifetime (110 fs) it is not possible to obtain an insightful vibrational spectral signature of this state.[52]

After passing the small excited-state barrier, crossing back to the ground-state potential energy surface[52−55] leads to the vibrationally coherent formation of a hot P_1 intermediate with retinal in a twisted 13-*cis* configuration, as well as vibrationally hot reactant. The associated coherence activity of the low-frequency modes (Figure 2a,b) suggests that the reaction coordinate is in fact not a simple normal mode but includes a superposition of several low-frequency modes, which also function as an internal heat sink to prevent coherent recrossing back to S_1.[56] Subsequent vibrational cooling with a time constant of 580 fs forms a stable P_1 product containing 13-*cis* retinal with an absorption maximum at 560 nm, which appears to persist for several hundreds of nanoseconds before it converts into the conductive P_2 intermediate.[11]

CONCLUSION

We used high time-resolution transient absorption spectroscopy to characterize the transient vibronic dynamics of *Ca*ChR1 from 500 to 900 nm after photoexcitation. The experimental results are consistent with the formation of the P_1 intermediate with a 110 fs time constant and subsequent vibrational relaxation with a 580 fs time constant. Broadband impulsive vibrational spectroscopy (BB-IVS) applied to the initial photoreaction of *Ca*ChR1 provides experimental evidence for an ultrafast photoisomerization of the retinal chromophore from an all-*trans* to a 13-*cis* configuration. Combining low-temperature resonance Raman spectroscopy with BB-IVS verified this assignment by revealing the 13-*cis* retinal with protonated Schiff base of the P_1 intermediate, formed in a vibrationally coherent fashion with a time constant of 110 fs.

The preliminary results presented here provide a base for more structurally sensitive investigations on the early dynamics of channelrhodopsins and similar molecules. In particular, time-resolved Raman studies[30,37,57] should be ideally suited to probe the cooling dynamics of *Ca*ChR1, promising to yield a much more refined picture of the relaxation dynamics.

ASSOCIATED CONTENT

Supporting Information

The Supporting Information is available free of charge on the ACS Publications website at DOI: 10.1021/jacs.5b12251. The data underpinning the results presented in this manuscript can be accessed free of charge at http://ora.ox.ac.uk.

Sample preparation, ultrafast spectroscopy, wavelength dependence of transient absorption dynamics, broadband impulsive vibrational spectroscopy (BB-IVS), resonance Raman spectroscopy at cryogenic temperature, comparison of vibrational difference spectra, comparison of transient dynamics in different rhodopsins, and linear prediction singular value decomposition analysis of low-frequency modes (PDF)

AUTHOR INFORMATION

Corresponding Authors

*philipp.kukura@chem.ox.ac.uk
*joachim.heberle@fu-berlin.de

Author Contributions

‖C.S. and V.M. contributed equally to this work.

Notes

The authors declare no competing financial interest.

ACKNOWLEDGMENTS

P.K. is supported by the EPSRC (EP/K006630/1). J.H. and R.S. acknowledge the financial support by the Deutsche Forschungsgemeinschaft (SFB 1078, projects B3 and B4, respectively). C.S. is supported by an EPSRC Doctoral Prize. We thank Dorothea Heinrich and Kirsten Hoffmann for technical assistance. D.E. thanks Ionela Radu for advice and discussion at an early stage of the project.

REFERENCES

(1) Wald, G. *Science* **1968**, *162*, 230.
(2) Liu, R. S.; Asato, A. E. *Proc. Natl. Acad. Sci. U. S. A.* **1985**, *82*, 259.
(3) Prigge, M.; Schneider, F.; Tsunoda, S. P.; Shilyansky, C.; Wietek, J.; Deisseroth, K.; Hegemann, P. *J. Biol. Chem.* **2012**, *287*, 31804.
(4) Hou, S. Y.; Govorunova, E. G.; Ntefidou, M.; Lane, C. E.; Spudich, E. N.; Sineshchekov, O. A.; Spudich, J. L. *Photochem. Photobiol.* **2012**, *88*, 119.
(5) Hegemann, P. *Annu. Rev. Plant Biol.* **2008**, *59*, 167.
(6) Hegemann, P.; Nagel, G. *EMBO Mol. Med.* **2013**, *5*, 173.
(7) Lórenz-Fonfría, V. A.; Heberle, J. *Biochim. Biophys. Acta, Bioenerg.* **2014**, *1837*, 626.
(8) Fenno, L.; Yizhar, O.; Deisseroth, K. *Annu. Rev. Neurosci.* **2011**, *34*, 389.
(9) Verhoefen, M. K.; Bamann, C.; Blöcher, R.; Förster, U.; Bamberg, E.; Wachtveitl, J. *ChemPhysChem* **2010**, *11*, 3113.
(10) Lórenz-Fonfría, V. A.; Schultz, B.-J.; Resler, T.; Schlesinger, R.; Bamann, C.; Bamberg, E.; Heberle, J. *J. Am. Chem. Soc.* **2015**, *137*, 1850.
(11) Muders, V.; Kerruth, S.; Lórenz-Fonfría, V. A.; Bamann, C.; Heberle, J.; Schlesinger, R. *FEBS Lett.* **2014**, *588*, 2301.

DOI: 10.1021/jacs.5b12251
J. Am. Chem. Soc. 2016, 138, 4757−4762

(12) Ernst, O. P.; Lodowski, D. T.; Elstner, M.; Hegemann, P.; Brown, L. S.; Kandori, H. *Chem. Rev.* **2014**, *114*, 126.
(13) Ogren, J. I.; Yi, A.; Mamaev, S.; Li, H.; Spudich, J. L.; Rothschild, K. J. *J. Biol. Chem.* **2015**, *290*, 12719.
(14) Ogren, J. I.; Yi, A.; Mamaev, S.; Li, H.; Lugtenburg, J.; DeGrip, W. J.; Spudich, J. L.; Rothschild, K. J. *Biochemistry* **2015**, *54*, 377.
(15) Sineshchekov, O. A.; Govorunova, E. G.; Wang, J.; Li, H.; Spudich, J. L. *Biophys. J.* **2013**, *104*, 807.
(16) Lórenz-Fonfría, V. A.; Muders, V.; Schlesinger, R.; Heberle, J. *J. Chem. Phys.* **2014**, *141*, 22D507.
(17) Johnson, P. J. M.; Halpin, A.; Morizumi, T.; Brown, L. S.; Prokhorenko, V. I.; Ernst, O. P.; Miller, R. J. D. *Phys. Chem. Chem. Phys.* **2014**, *16*, 21310.
(18) Rozin, R.; Wand, A.; Jung, K.-H.; Ruhman, S.; Sheves, M. *J. Phys. Chem. B* **2014**, *118*, 8995.
(19) Liebel, M.; Schnedermann, C.; Bassolino, G.; Taylor, G.; Watts, A.; Kukura, P. *Phys. Rev. Lett.* **2014**, *112*, 238301.
(20) Mathies, R. A.; Brito Cruz, C.; Pollard, W. T.; Shank, C. V. *Science (Washington, DC, U. S.)* **1988**, *240*, 777.
(21) Neumann-Verhoefen, M. K.; Neumann, K.; Bamann, C.; Radu, I.; Heberle, J.; Bamberg, E.; Wachtveitl, J. *J. Am. Chem. Soc.* **2013**, *135*, 6968.
(22) Schapiro, I.; Ruhman, S. *Biochim. Biophys. Acta, Bioenerg.* **2014**, *1837*, 589.
(23) Cheminal, A.; Léonard, J.; Kim, S.-Y.; Jung, K.-H.; Kandori, H.; Haacke, S. *Phys. Chem. Chem. Phys.* **2015**, *17* (38), 25429.
(24) Schoenlein, R. W.; Peteanu, L. A.; Mathies, R. A.; Shank, C. V. *Science* **1991**, *254*, 412.
(25) Johnson, P. J. M.; Halpin, A.; Morizumi, T.; Prokhorenko, V. I.; Ernst, O. P.; Miller, R. J. D. *Nat. Chem.* **2015**, *7*, 980.
(26) Schnedermann, C.; Liebel, M.; Kukura, P. *J. Am. Chem. Soc.* **2015**, *137*, 2886.
(27) Stensitzki, T.; Muders, V.; Schlesinger, R.; Heberle, J.; Heyne, K. *Front. Mol. Biosci.* **2015**, *2*, 41.
(28) Liebel, M.; Kukura, P. *J. Phys. Chem. Lett.* **2013**, *4*, 1358.
(29) Musser, A. J.; Liebel, M.; Schnedermann, C.; Wende, T.; Kehoe, T. B.; Rao, A.; Kukura, P. *Nat. Phys.* **2015**, *11*, 352.
(30) Liebel, M.; Schnedermann, C.; Wende, T.; Kukura, P. *J. Phys. Chem. A* **2015**, *119*, 9506.
(31) Dexheimer, S. L.; Wang, Q.; Peteanu, L. A.; Pollard, W. T.; Mathies, R. A.; Shank, C. V. *Chem. Phys. Lett.* **1992**, *188*, 61.
(32) Ruhman, S.; Kohler, B.; Joly, A. G.; Nelson, K. A. *IEEE J. Quantum Electron.* **1988**, *24*, 470.
(33) Ruhman, S.; Joly, A. G.; Nelson, K. A. *IEEE J. Quantum Electron.* **1988**, *24*, 460.
(34) Dobryakov, A. L.; Ernsting, N. P. *J. Chem. Phys.* **2008**, *129*, 184504.
(35) Pollard, W. T.; Dexheimer, S. L.; Wang, Q.; Peteanu, L. A.; Shank, C. V.; Mathies, R. A. *J. Phys. Chem.* **1992**, *96*, 6147.
(36) Kumar, A. T. N.; Rosca, F.; Widom, A.; Champion, P. M. *J. Chem. Phys.* **2001**, *114*, 701.
(37) Wende, T.; Liebel, M.; Schnedermann, C.; Pethick, R. J.; Kukura, P. *J. Phys. Chem. A* **2014**, *118*, 9976.
(38) Wang, Q.; Schoenlein, R. A.; Peteanu, L. A.; Mathies, R. A.; Shank, C. V. *Science* **1994**, *266*, 422.
(39) Braiman, M.; Mathies, R. A. *Proc. Natl. Acad. Sci. U. S. A.* **1982**, *79*, 403.
(40) Smith, S. O.; Pardoen, J. A.; Lugtenburg, J.; Mathies, R. A. *J. Phys. Chem.* **1987**, *91*, 804.
(41) Gai, F.; Hasson, K. C.; McDonald, J. C.; Anfinrud, P. A. *Science* **1998**, *279*, 1886.
(42) Althaus, T.; Eisfeld, W.; Lohrmann, R.; Stockburger, M. *Isr. J. Chem.* **1995**, *35*, 227.
(43) Weidlich, O.; Ujj, L.; Jäger, F.; Atkinson, G. H. *Biophys. J.* **1997**, *72*, 2329.
(44) Kawaguchi, S.; Kambara, O.; Shibata, M.; Kandori, H.; Tominaga, K. *Phys. Chem. Chem. Phys.* **2010**, *12*, 10255.
(45) Kraack, J. P.; Buckup, T.; Motzkus, M. *Phys. Chem. Chem. Phys.* **2011**, *13*, 21402.
(46) Zgrablić, G.; Haacke, S.; Chergui, M. *Chem. Phys.* **2007**, *338*, 168.
(47) Kraack, J. P.; Buckup, T.; Motzkus, M. *Phys. Chem. Chem. Phys.* **2012**, *14*, 13979.
(48) Fuß, W. *Chem. Phys.* **2013**, *425*, 96.
(49) Seidner, L.; Domcke, W. *Chem. Phys.* **1994**, *186*, 27.
(50) Luk, H. L.; Melaccio, F.; Rinaldi, S.; Gozem, S.; Olivucci, M. *Proc. Natl. Acad. Sci. U. S. A.* **2015**, *112*, 15297.
(51) Dokukina, I.; Weingart, O. *Phys. Chem. Chem. Phys.* **2015**, *17*, 25142.
(52) Liebel, M.; Schnedermann, C.; Kukura, P. *Phys. Rev. Lett.* **2014**, *112*, 198302.
(53) Polli, D.; Altoè, P.; Weingart, O.; Spillane, K. M.; Manzoni, C.; Brida, D.; Tomasello, G.; Orlandi, G.; Kukura, P.; Mathies, R. A.; Garavelli, M.; Cerullo, G. *Nature* **2010**, *467*, 440.
(54) Sovdat, T.; Bassolino, G.; Liebel, M.; Schnedermann, C.; Fletcher, S. P.; Kukura, P. *J. Am. Chem. Soc.* **2012**, *134*, 8318.
(55) Bassolino, G.; Sovdat, T.; Liebel, M.; Schnedermann, C.; Odell, B.; Claridge, T. D. W.; Kukura, P.; Fletcher, S. P. *J. Am. Chem. Soc.* **2014**, *136*, 2650.
(56) Kühl, A.; Domcke, W. *J. Chem. Phys.* **2002**, *116*, 263.
(57) Kukura, P.; McCamant, D. W.; Yoon, S.; Wandschneider, D. B.; Mathies, R. A. *Science* **2005**, *310*, 1006.

DOI: 10.1021/jacs.5b12251
J. Am. Chem. Soc. 2016, 138, 4757−4762